Reinforced Lattice Kalman Filters: A Robust Nonlinear Estimation Strategy

Abolfazl Rahimnejad, *Member, IEEE,* Javad Enayati, Luigi Vanfretti, *Senior Member, IEEE,* Stephen Andrew Gadsden, *Senior Member, IEEE,* Mohammad AlShabi, *Senior Member, IEEE*

***Abstract*— This paper introduces the Sliding Innovation Lattice Filter (SILF), a robust extension of the Lattice Kalman Filter (LKF) that leverages sliding mode theory. SILF incorporates a sliding boundary layer in the measurement update formulation, enabling the filter innovation to slide within predefined upper and lower bounds. This enhances the robustness of SILF, making it resilient to model uncertainties and noise. Additionally, a derivative-free formulation of SILF is developed using statistical linear regression, eliminating the need for Jacobian calculations. To further improve accuracy, robustness, and convergence behavior in the presence of abrupt changes in system model/parameters, SILF is reinforced with the Iterated Sigma Point Filtering and Strong Tracking Filtering strategies, resulting in the Reinforced Lattice Kalman Filter (RLKF). The experimental findings for the estimation of distorted power waveforms illustrate the superior performance of SILF and RLKF over competing methods, especially when operating in scenarios characterized by model uncertainties and noisy environments.**

***Index Terms*—Lattice Kalman filter, Variable structure filter, Adaptive fading factor, iterated filtering method, Robust estimators.**

I. Introduction

Estimation algorithms play an essential role in the smooth and efficient operation and control of the system in many science and engineering fields. In recent decades, many research works have focused on the development of accurate and robust estimators based on the best-known Kalman filter (KF) algorithm [1] in the presence of model nonlinearity and uncertainty. KF is formulated as a predictor-corrector estimator, in the framework of linear Bayesian filtering with Gaussian assumption based on the derivation of the optimal solution for Kalman gain (used in the correction stage) that minimizes the trace of the posterior (updated) state error covariance matrix. However, the real-world systems most often present model nonlinearity that requires an efficient extension of KF in terms of accuracy and complexity. The nonlinear extensions of KF utilize either the derivative-based linearization method (based on Jacobian matrix calculation) as per extended KF (EKF) [2], [3] or the derivative-free methods (based on statistical linear regression or numerical integration) as per the sigma point KF (UKF) [4], [5], cubature KF (CKF) [6], Lattice KF (KF) [7], etc. Other than model nonlinearity, in most practical applications, the system is exposed to uncertainties originating in model changes (under different operating conditions) and/or noise behavior, which directly yields a declined performance or failure (divergence) of the KF-based algorithms. To address this issue, a couple of strategies have been proposed in the literature for improving the filter's robustness in the context of both linear and nonlinear Kalman filtering. A robust version of KF is proposed in [8] by introducing an adaptive fading factor that puts more weight on the most recent observations in the presence of modeling mismatch. Being inspired by the strategy proposed in [8], authors in [9], [10] propose the strong tracking filtering method to increase the robustness of nonlinear filtering algorithms including UKF and CKF. As another robust extension of KF algorithms, the H-infinity filter [11] and its hybrid nonlinear variants [12]–[14] are proposed in the framework of the minimax estimation method in which the worst-case estimation error is minimized (as opposed to minimization of mean squared error (MSE) by KF). Although the H-infinity filter improves the estimation results in an uncertain environment, the level of improvement is highly sensitive to how its parameters are tuned and it adds some computational complexity to the original KF [11]. Inspired by the concept of sliding mode control theory and sliding mode observer, the Variable structure filter (VSF) was formulated to improve the robustness of the KF [15], whose extension for nonlinear systems under Gaussian assumption, including smooth variable structure filter (SVSF) and time-varying SVSF [16], were later developed to maintain states within a bounded tube in the presence of uncertainty resources. Comparative results indicate that SVSF outperforms the well-known EKF, UKF, and CKF algorithms under uncertain and noisy

This paper was submitted for review on March 3, 2023 with support from the Natural Sciences and Engineering Research Council of Canada (NSERC) Discovery Grant.

A. Rahimnejad and S. A. Gadsden are with the Faculty of Engineering at the McMaster University, Hamilton, Ontario, Canada (e-mails: a.rahimnejad@mcmaster.ca and gadsden@mcmaster.ca).

J. Enayati is with R&D Department, Mazinoor Lighting Industry, Babol, Mazandaran, Iran. (e-mail: j.enayati@mazinoor.com).

L. Vanfretti is with Computer and Systems Engineering Department at Rensselaer Polytechnic Institute, Troy, New York, U.S.A. (e-mail: luigi.vanfretti@gmail.com).

M. Al-Shabi is with the Department of Mechanical and Nuclear Engineering at University of Sharjah, Sharjah, UAE (e-mail: malshabi@sharjah.ac.ae).

environments [17]–[19]. Moreover, to further improve the performance of SVSF, authors in [19] develops some hybridization of SVSF with nonlinear KF such as UKF and CKF among the others, and the obtained results show the better performance of CKF-SVSF. In order to reduce the computational burden of SVFS and improve its accuracy as well, a new variant of VSF called the sliding innovation filter (SIF) along with its derivative-based nonlinear extension, namely as extended SIF (ESIF) have been formulated for Gaussian linear and nonlinear systems under uncertainties, respectively [20], [21]. To improve the performance of SIF/ESIF against higher level of uncertainty and nonlinearity, a hybridized version of SIF combined with particle filter (PFSIF) and CKF (SICF) have been formulated in [22] and [23], respectively. An adaptive formulation of Particle Filter (PF) which carries out sampling based on randomized Quasi-Monte Carlo (QMC) technique has been presented in [24]. A robust and adaptive formulation of H-infinity filter utilizing adaptive fading factor strategy has been proposed in [25].

In our previous work [7], we have proposed a new nonlinear filtering strategy based on a class of QMC integration methods, called lattice rules, to approximate Gaussian-weighted multi-dimensional integrals in the nonlinear KF framework using low discrepancy lattice points. This nonlinear filtering approach established is based on the Korobov type rank-1 lattice rule is referred to as lattice Kalman filter (LKF) [26]. The main superiority of the LKF over other sigma point filtering methods has been recognised to be its relatively low computational complexity (due to a reduced number of sampling points) while maintaining accuracy at an asymptotically same level. However, the accuracy and robustness of the LKF, particularly with a low number of sampling points, diminish when confronted with highly nonlinear and uncertain systems. To address these challenges, this paper proposes a novel and robust formulation of the LKF specifically designed for nonlinear systems operating under high levels of uncertainties and nonlinearity. The main contributions of the proposed algorithm can be listed as follows:

1) Exploitation of the sliding innovation strategy presented in [21], combined with lattice-based generated sampling points with an adjustable number of points. This integration gives rise to the sliding innovation lattice filter (SILF), which significantly improves the robustness of the original LKF.

2) Development of a derivative-free formulation of SILF based on the statistical linearization approach. This formulation enables SILF to effectively handle highly nonlinear systems without the need for computationally expensive Jacobian matrix calculations.

3) Integration of the iterated filtering algorithm [27]–[29] to enhance the accuracy of SILF. The iterative nature of this algorithm refines the estimation results and improves their overall accuracy.

4) Incorporation of the adaptive fading factor introduced by the strong tracking filter theory. This inclusion leads to a reformulation of the measurement update equations, resulting in improved convergence behavior and performance of SILF, particularly in scenarios involving abrupt changes in the system model/parameters.

The combination of iterated strategy and strong tracking filter applied to the derivative-free SILF method is called reinforced lattice Kalman filter (RLKF). The proposed SILF and RLKF are then employed to estimate the distorted electrical waveforms of the power grids in four different scenarios including static, dynamic, transient operation of the system, and real-time application as well. Simulation and experimental results demonstrate the superiority of the proposed methods in terms of estimation accuracy and robustness against uncertain system models and noise disturbances, with RLKF presenting better results, especially for estimation under uncertainty, but at a higher computational time. This complexity, however, can be addressed by reducing the number of sampling points (inherited by the lattice rule) of RLKF to some extent.

The rest of the paper is organized as follows: In section II, we briefly overview the main concept and formulation of the LKF method followed by the proposed robust formulation of LKF in section III. The sliding innovation lattice filter (SILF), iterated version of SILF augmented with a strong tracking filter method is presented in section III, where at the end, the proposed reinforced LKF (RLKF) is formulated. Different simulations and experiments, which are designed in the framework of harmonic estimation problems in power systems, to evaluate the performance of the proposed filter along with the corresponding results are discussed in section IV. Finally, section V concludes the main outcomes of the paper and discusses future works.

II. Lattice Kalman Filter

In [7], we employed the rank-1 lattice rule [30] to generate low-discrepancy points to approximate multivariate integrals in the nonlinear Kalman filtering framework to propose the lattice Kalman filter (LKF) whose main concept and formulation are briefly overviewed in this section.

LKF is formulated in the Gaussian filtering framework for a system with noisy nonlinear dynamics whose process and measurement model are defined as follows:

$$x_k = f\ (x_{k-1}, u_{k-1}) + w_k \qquad (1)$$

$$z_k = h\ (x_k) + v_k \qquad (2)$$

where w_k and v_k represents the process and measurement noises, respectively, and assumed to be independent and have Gaussian distributions with zero mean and covariance matrices Q and R, respectively. The main concept behind LKF formulation is to approximate the multivariate Gaussian weighted integrals, associated with the recursive calculation of mean and covariance of conditional density at the current time step, using lattice rule-based generated sampling points [31], [32]. Consequently, LKF, as a predictor-corrector estimator is formulated as per the following stages:

A. Prediction Stage:

The prior state estimate $\hat{x}_{k|k-1}$ and state error covariance matrix $P_{k|k-1}$ at the kth recursion step can be calculated as per the following equations, respectively:

$$\hat{x}_{k|k-1} \approx \frac{1}{N}\sum_{j=0}^{N-1} f\left(X_{j,k-1|k-1}^{QGL}, u_{k-1}\right) \quad (3)$$

$$P_{xx,k|k-1} \approx \frac{1}{N}\sum_{j=0}^{N-1} \left[f\left(X_{j,k-1|k-1}^{QGL}, u_{k-1}\right) - \hat{x}_{k|k-1}\right] * \left[f\left(X_{j,k-1|k-1}^{QGL}, u_{k-1}\right) - \hat{x}_{k|k-1}\right]^T + Q_{k-1} \quad (4)$$

where N is the number of sampling points, and $X_{j,k-1|k-1}^{QGL}; j = 0,1,\dots,N-1$ denotes quasi-Gaussian lattice points that are generated using the procedure presented in (5):

$$\begin{aligned} P_{xx,k-1|k-1} &= S_{k-1|k-1}^T S_{k-1|k-1} \\ X_j^{SN,QL} &= \phi^{-1}\left(x_{j,d^*}^{L,Shifted}\right);\ j = 0,1,2,\dots,N-1 \\ X_{j,k-1|k-1}^{QGL} &= \hat{x}_{k-1|k-1} + S_{k-1|k-1} X_j^{SN,QL}; j = 0,\dots,N-1 \end{aligned} \quad (5)$$

In which $\hat{x}_{k-1|k-1}$ and $P_{k-1|k-1}$ are the previous posterior mean and covariance matrix, respectively, and $S_{k-1|k-1}$ is calculated by applying Cholesky factorization to the posterior covariance matrix at the previous time step $P_{xx,k-1|k-1}$. Also, $\phi^{-1}(.)$ represents inverse normal cumulative distribution function evaluated at the shifted lattice points with a random permutation $x_{j,d^*}^{L,Shifted};\ j = 0,1,2,\dots,N-1$ that is generated in the unit hypercube using the following procedure. Firstly, randomly shifted lattice points are produced as follows:

$$x_j^{L,Shifted} = \left(\frac{G\ j\ mod\ N}{N} + \Delta\right) mod\ 1\ ; \quad j = 0,\dots,N-1 \quad (6)$$

where Δ is a random shift vector, generated based on the Cranely Patterson shift strategy [33], and is applied to the Korobov type rank-1 lattice points; G represents the generating vector, defined as follows as per the Korobov type lattice rule [34]:

$$G = [1\ c\ c^2\ \dots\ c^{d-1}]^T \quad (7)$$

Moreover, $mod\ 1$ denoted in (6) produces modular 1 of the term inside the round brackets and operates element-wise. Note that in (7), we have to choose c so as to be a coprime integer with N.

Additionally, in this paper, to prevent the probable bias originating in the dependency of a certain state/dimension on the outcome of resampling (in different time steps), a random permutation of lattice points over the dimensions is applied to the points generated in (6) $x_j^{L,Shifted}$ which results in a new point set $x_{d^*}^{L,Shifted}$ where d^* denotes the uniform and random permutation of the points over the problem dimension d (random permutation of integers in $[1\ 2\ \dots\ d]$). This way $x_{d^*}^{L,Shifted}$ is generated in each recursion independently.

B. Correction stage

In this stage, the quasi-Gaussian lattice points are updated using the prior state estimate $\hat{x}_{k|k-1}$ and covariance matrix $P_{xx,k|k-1}$ using the same procedure defined in (5) reformulated as follows:

$$\begin{aligned} P_{xx,k|k-1} &= S_{k|k-1}^T S_{k|k-1} \\ X_j^{SN,QL} &= \phi^{-1}\left(x_{j,d^*}^{L,Shifted}\right);\ j = 0,1,2,\dots,N-1 \\ X_{j,k|k-1}^{QGL} &= \hat{x}_{k|k-1} + S_{k|k-1} X_j^{SN,QL}; j = 0,1,2,\dots,N-1 \end{aligned} \quad (8)$$

The updated points $X_{j,k|k-1}^{QGL}; j = 0,1,\dots,N-1$ are then used to calculate the predicted measurement vector, and innovation and cross-covariance matrices using the equations (9) through (11), respectively:

$$\hat{z}_{k|k-1} \approx \frac{1}{N}\sum_{j=0}^{N-1} h\left(X_{j,k|k-1}^{QGL}, u_k\right) \quad (9)$$

$$P_{zz,k|k-1} \approx \frac{1}{N}\sum_{j=0}^{N-1} \left[h\left(X_{j,k|k-1}^{QGL}, u_k\right) - \hat{z}_{k|k-1}\right] * \left[h\left(X_{j,k|k-1}^{QGL}, u_k\right) - \hat{z}_{k|k-1}\right]^T + R_k \quad (10)$$

$$P_{xz,k|k-1} \approx \frac{1}{N}\sum_{j=0}^{N-1} \left[X_{j,k|k-1}^{QGL} - \hat{x}_{k|k-1}\right] * \left[h\left(X_{j,k|k-1}^{QGL}, u_k\right) - \hat{z}_{k|k-1}\right]^T \quad (11)$$

Eventually, the LKF gain G_k, the posterior state estimate $\hat{x}_{k|k}$, and (state) error covariance matrix $P_{xx,k|k}$ can be computed using the following equations, respectively:

$$G_k = P_{xz,k|k-1} P_{zz,k|k-1}^{-1} \quad (12)$$

$$\hat{x}_{k|k} = \hat{x}_{k|k-1} + G_k\left(z_k - \hat{z}_{k|k-1}\right) \quad (13)$$

$$P_{xx,k|k} = P_{xx,k|k-1} - G_k P_{zz,k|k-1} G_k^T \quad (14)$$

III. Proposed robust reformulation of LKF

As per our previous work [7], LKF yielded asymptotically similar results to UKF but with less computational effort. This lower computational burden originates in the adjustably lower number of sampling points (for the systems with a lower level of nonlinearity and uncertainty) introduced by the lattice-based integration method. However, the accuracy and robustness of LKF decline in the presence of severe nonlinearity, modeling uncertainty, and high-level noise disturbances. This issue becomes even worse when a lower number of sampling points compared to that of the other sigma-point methods is used to approximate the nonlinear integrals. This shortfall against highly nonlinear models and model uncertainties and disturbances has motivated us to propose a robust formulation of LKF which is presented and formulated in the following subsections.

A. *Sliding Innovation Lattice Filter (SILF)*

The first modification applied to LKF is founded on the sliding innovation strategy that is inspired by the concept of sliding mode observer and smooth variable structure filter (SVSF) [21]. In this regard, the time update stage of the proposed SILF algorithm is formulated similar to LKF; however, unlike LKF (nonlinear KF, in general) whose gain is derived as a function of the state error covariances, the measurement update equations of SILF are developed as if the gain is a function of the innovation vector sliding within a targeted hyper-tube (high-dimensional tube). If the innovation term is denoted as $\tilde{z}_{k|k-1} = z_k - \hat{z}_{k|k-1}$, the SILF gain at the current time step G_k can be formulated as per the following equation:

$$G_k^{silf} = H_k^{pinv} Sat^{diag}\left(\frac{|\tilde{z}_{k|k-1}|}{\delta}\right) \tag{15}$$

In this formulation, H_k^{pinv} represents pseudoinverse of the measurement matrix H_k, Sat^{diag} represents the diagonal matrix of saturation function applied to the element-wise division of the absolute value of the innovation vector by a control vector δ; this keeps the gain inside the targeted boundary layers (hyper-tube). Note that saturation function Sat yields its output sliding between +1 and -1. Based on the level of uncertainties in the estimation process, the sliding boundary layer width δ can be determined [21].

Since the measurement equation is often nonlinear in the real-world problems, the nonlinear measurement function $h(x_k)$ can be either approximated by analytical linearization based on calculating the Jacobian matrix (derivative-based formulation) or formulated using statistical linear regression (derivative-free formulation); the latter is developed for the proposed SILF in this paper (derivative-free SILF) which is further discussed in the following subsection:

- *Derivative-free SILF*

It can be shown that for highly nonlinear measurement models, linearization using the first term of the Taylor series around the operating point would lead to inaccurate approximation. On the other hand, although the approximation of nonlinear models using the higher-order terms of Taylor series expansion yields a more accurate result, its high computational complexity is a substantial barrier in real-time applications. Therefore, in order to relax the calculation of the Jacobians matrix and the required smoothness of the nonlinear functions, we employ the statistical linear regression method [35] to develop a derivative-free SILF formulation.

If we use the lattice-based generated sampling points to linearize the nonlinear measurement function using statistical regression as per the following equation,

$$z_k = H_k x_k + b_k + \mathbb{e}_k \tag{16}$$

then, the parameters of the linearized model H_k and b_k can be obtained by minimizing the mean squared error (MSE) of the linear regression model:

$$H_k = P_{xz,k|k-1}^T P_{xx,k|k-1}^{-1} \tag{17}$$

$$b_k = z_k - H_k x_{k|k-1} + \mathbb{e}_k \tag{18}$$

and deviation of statistical linear regression model $\mathbb{e}_k$ is a stochastic variable with zero mean and covariance of $P_{zz,k|k-1} - H_k P_{xx,k|k-1} H_k^T$. In this framework, we can obtain the pseudo-inverse of statistically linearized H_k by applying the Moore-Penrose formula to (17):

$$H_k^{pinv} = P_{xx,k|k-1}^T \left(P_{xz,k|k-1} P_{xz,k|k-1}^T\right)^{-1} P_{xz,k|k-1} \tag{19}$$

Note that in this study, we use the derivative-free formulation of H_k^{pinv} presented in (19) to calculate the SILF gain G_k^{silf} (15) using which state estimates and state covariance matrices are updated as per the following equations:

$$\hat{x}_{k|k} = \hat{x}_{k|k-1} + G_k^{silf} \tilde{z}_{k|k-1} \tag{20}$$

$$P_{xx,k|k} = P_{xx,k|k-1} - G_k^{silf} P_{zz,k|k-1} {G_k^{silf}}^T \tag{21}$$

For the rest of this study, when we use the term SILF, we technically refer to the derivative-free formulation of SILF.

B. *Iterated SILF*

To improve the estimation accuracy of the proposed SILF algorithm, the iterated sigma-point filtering concept [27] is utilized to formulate iterated SILF (ISILF). The main idea of the iterated filtering strategy is behind the fact that the updated state estimates $\hat{x}_{k|k}$ is expected to provide a better estimate than the predicted state estimates $\hat{x}_{k|k-1}$, because $\hat{x}_{k|k}$ is calculated once the most recent measured data at time step k is received. We exploit this fact to regenerate quasi-Gaussian lattice points using the updated state estimate $\hat{x}_{k|k}$ and error covariance matrix $P_{xx,k|k}$, based on (8), which are then used to recalculate statistical moments of the posterior state density denoted as $\hat{x}_{k|k}^{(iter)}$ and $P_{xx,k|k}^{(iter)}$ at the current time step k and iteration count $iter$. This strategy may yield a decline in the errors introduced by employed numerical integration and statistical regression methods after a specific number of iterations. The proposed ISILF adds additional stages to the original SILF defined as follows.

After calculating $\hat{x}_{k|k}$ and $P_{xx,k|k}$ in each time step k, we initialize $\hat{x}_{k|k}^{(0)} = \hat{x}_{k|k-1}$, $P_{xx,k|k}^{(0)} = P_{xx,k|k-1}$, $\hat{x}_{k|k}^{(1)} = \hat{x}_{k|k}$, $P_{xx,k|k}^{(1)} = P_{xx,k|k}$, and set $iter = 2$. We then calculate the new quasi-Gaussian lattice points as follows:

$$P_{xx,k|k}^{(iter-1)} = {S_{k|k}^{(iter-1)}}^T S_{k|k}^{(iter-1)}$$

$$X_j^{SN,QL} = \phi^{-1}\left(x_{j,d^*}^{L,Shifted}\right);\ j = 0, 1, 2, \dots, N-1$$

$$X_{j,k|k}^{QGL\,(iter)} = \hat{x}_{k|k}^{(iter-1)} + S_{k|k}^{(iter-1)} X_j^{SN,QL};\ j = 0, \dots, N-1 \tag{22}$$

The newly generated sampling points are then used to correct the measurement update equations as follows:

$$\hat{x}_{k|k-1}^{(iter)} \approx \frac{1}{N}\sum_{j=0}^{N-1} f\left(X_{j,k|k}^{QGL\,(iter)}, u_{k-1}\right) \quad (23)$$

$$\hat{z}_{k|k-1}^{(iter)} \approx \frac{1}{N}\sum_{j=0}^{N-1} h\left(X_{j,k|k}^{QGL\,(iter)}, u_{k}\right) \quad (24)$$

$$P_{zz,k|k-1}^{(iter)} \approx \frac{1}{N}\sum_{j=0}^{N-1} \left[h\left(X_{j,k|k}^{QGL\,(iter)}, u_k\right) - \hat{z}_{k|k-1}^{(iter)}\right] * \left[h\left(X_{j,k|k}^{QGL\,(iter)}, u_k\right) - \hat{z}_{k|k-1}^{(iter)}\right]^T + R_k \quad (25)$$

$$P_{xz,k|k-1}^{(iter)} \approx \frac{1}{N}\sum_{j=0}^{N-1} \left[X_{j,k|k}^{QGL\,(iter)} - \hat{x}_{k|k-1}^{(iter)}\right] * \left[h\left(X_{j,k|k}^{QGL\,(iter)}, u_k\right) - \hat{z}_{k|k-1}^{(iter)}\right]^T \quad (26)$$

$$G_k^{silf\,(iter)} = H_k^{pinv\,(iter)} Sat^{diag}\left(\frac{\left|z_k - \hat{z}_{k|k-1}^{(iter)}\right|}{\delta}\right) \quad (27)$$

where

$$H_k^{pinv\,(iter)} = P_{xx,k|k}^{(iter-1)}\left(P_{xz,k|k-1}^{(iter)}\left(P_{xz,k|k-1}^{(iter)}\right)^T\right)^{-1} P_{xz,k|k-1}^{(iter)} \quad (28)$$

Eventually, the state mean and error covariance matrix at each iteration are updated as follows:

$$\hat{x}_{k|k}^{(iter)} = \hat{x}_{k|k-1}^{(iter)} + G_k^{silf\,(iter)} \tilde{z}_{k|k-1}^{(iter)} \quad (29)$$

$$P_{xx,k|k}^{(iter)} = P_{xx,k|k}^{(iter-1)} - G_k^{silf\,(iter)} P_{zz,k|k-1}^{(iter)} (G_k^{silf\,(iter)})^T \quad (30)$$

It can be easily proven that the convergence of ISILF is guaranteed with the proceed of iterations, as per the discussion presented in section II.C of [27]. However, as the number of iterations increases to achieve better accuracy, the computational complexity introduced by the iterative strategy also increases. Note that for most real-world problems a noticeable improvement in accuracy is obtained after only a few numbers of iterations (in most cases one or two iterations) [29].

C. Strong Tracking Filtering Strategy

To further improve the robustness of the proposed SILF against abrupt changes in the system dynamics, the strong tracking filtering strategy, originally proposed in [10], is used to introduce an adaptive fading factor to the predicted covariance matrix $P_{xx,k|k-1}$ of SILF algorithm. This strategy, in fact, reduces the weight of the old measurements against that of the recent ones. The adaptive fading factor, denoted as λ_k, can be calculated as follows (recall $\tilde{z}_{k|k-1} = z_k - \hat{z}_{k|k-1}$):

$$\lambda_k = max\{c_k, 1\} \quad (31)$$

$$c_k = \frac{trace(N_k)}{trace(M_k)} \quad (32)$$

$$N_k = E_k^{\tilde{z}} - P_{xz,k|k-1}^T P_{xx,k|k-1}^{-1} Q_{k-1} P_{xx,k|k-1} P_{xz,k|k-1}^T - \beta R_k \quad (33)$$

$$M_k = P_{zz,k|k-1} - E_k^{\tilde{z}} + N_k + (\beta - 1)R_k \quad (34)$$

$$E_k^{\tilde{z}} = \mathbb{E}\{\tilde{z}_{k|k-1}\,\tilde{z}_{k|k-1}^T\} = \begin{cases} \tilde{z}_{k|k-1}\,\tilde{z}_{k|k-1}^T & ; k = 0 \\ \dfrac{\rho E_{k-1}^{\tilde{z}} + \tilde{z}_{k|k-1}\,\tilde{z}_{k|k-1}^T}{1+\rho} & ; k > 0 \end{cases} \quad (35)$$

where ρ is the forgetting factor and β is the softening factor which are usually set to 0.95 and 4.5, respectively. Then, λ_k is applied to correct $P_{xx,k|k-1}$ at time step k as per the following equation [10]:

$$P_{xx,k|k-1}^{ST} = \lambda_k\left(P_{xx,k|k-1} - Q_{k-1}\right) + Q_{k-1} \quad (36)$$

in which subscript ST stands for strong tracking. $P_{xx,k|k-1}^{ST}$ is then used to calculate new quasi-gaussian lattice points based on (8), which are used to reformulate the update stage of SILF.

D. Reinforced Lattice Kalman Filter (RLKF)

Eventually, we employ the three abovementioned algorithms simultaneously to propose a new accurate and robust version of LKF, named reinforced LKF (RLKF), which exploits the guaranteed stability of the sliding innovation strategy, boosted robustness against abrupt changes in system dynamics of the strong tracking filtering strategy (by defining adaptive fading factor applied to the predicted state error covariance), and improved accuracy guaranteed by iterative sigma-point filtering algorithm. The stages and flowchart of the proposed RLKF algorithm are presented in Table I and Fig. 1, respectively.

IV. Simulations and Experimental Setup

In this section, the accuracy, robustness, and computational complexity of the proposed filters, SILF and RLKF (strong tracking strategy combined with iterative SILF), are evaluated. For this purpose, the proposed filtering methods are applied to estimate the harmonic parameters (amplitudes and phases of the harmonic contents) of distorted waveforms in power grids. Sate vector for the harmonic estimation problems is generally defined as follows:

$$x = [\varphi_1, \varphi_2, \dots, \varphi_r, Amp_1, Amp_2, \dots Amp_r]^T \quad (37)$$

where Amp_r and φ_r are the amplitude and phase of the r-th harmonic order, respectively. Note that the dimension of the vector state is $n = 2 * r$. Then, the system and measurement models are defined as per the following equations, respectively:

$$x_k = I_{n\times n} * x_{k-1} + w_{k-1} \quad (38)$$

$$z_k = \left(\sum_{i=1}^{r} Amp_i * \sin(\varphi_r)\right) + v_k \quad (39)$$

TABLE I
THE STAGES OF THE PROPOSED RLKF ALGORITHM

Initialization:	$\hat{x}_{k-1\|k-1} = \hat{x}_0$
	$P_{xx,k-1\|k-1} = P_{xx,0} = \mathrm{E}\{(x_0 - \hat{x}_0)(x_0 - \hat{x}_0)^T\}$
State prediction:	$P_{xx,k-1\|k-1} = S_{k-1\|k-1}^T S_{k-1\|k-1}$
	$X_j^{SN,QL} = \phi^{-1}\left(x_{j,d^*}^{L,Shifted}\right);\ j = 0, 1, 2, \dots, N-1$
	$X_{j,k-1\|k-1}^{QGL} = \hat{x}_{k-1\|k-1} + S_{k-1\|k-1} X_j^{SN,QL}\ ; j = 0, 1, 2, \dots, N-1$
	$\hat{x}_{k\|k-1} \approx \frac{1}{N}\sum_{j=0}^{N-1} f\left(X_{j,k-1\|k-1}^{QGL}, u_{k-1}\right)$
	$P_{xx,k\|k-1} \approx \frac{1}{N}\sum_{j=0}^{N-1} \left[f\left(X_{j,k-1\|k-1}^{QGL}, u_{k-1}\right) - \hat{x}_{k\|k-1}\right]$
	$* \left[f\left(X_{j,k-1\|k-1}^{QGL}, u_{k-1}\right) - \hat{x}_{k\|k-1}\right]^T + Q_{k-1}$
Measurement prediction:	$P_{xx,k\|k-1} = S_{k\|k-1}^T S_{k\|k-1}$
	$X_j^{SN,QL} = \phi^{-1}\left(x_{j,d^*}^{L,Shifted}\right);\ j = 0, 1, 2, \dots, N-1$
	$X_{j,k\|k-1}^{QGL} = \hat{x}_{k\|k-1} + S_{k\|k-1} X_j^{SN,QL}\ ; j = 0, 1, 2, \dots, N-1$
	$\hat{z}_{k\|k-1} \approx \frac{1}{N}\sum_{j=0}^{N-1} h\left(X_{j,k\|k-1}^{QGL}, u_k\right)$
	$P_{zz,k\|k-1} \approx \frac{1}{N}\sum_{j=0}^{N-1} \left[h\left(X_{j,k\|k-1}^{QGL}, u_k\right) - \hat{z}_{k\|k-1}\right]$
	$* \left[h\left(X_{j,k\|k-1}^{QGL}, u_k\right) - \hat{z}_{k\|k-1}\right]^T + R_k$
	$P_{xz,k\|k-1} \approx \frac{1}{N}\sum_{j=0}^{N-1} \left[X_{j,k\|k-1}^{QGL} - \hat{x}_{k\|k-1}\right]$
	$* \left[h\left(X_{j,k\|k-1}^{QGL}, u_k\right) - \hat{z}_{k\|k-1}\right]^T$
	$\tilde{z}_{k\|k-1} = z_k - \hat{z}_{k\|k-1}$
Adaptive fading factor:	$E_k^{\tilde{z}} = \begin{cases} \tilde{z}_{k\|k-1}\ \tilde{z}_{k\|k-1}^T & ; k = 0 \\ \dfrac{\rho E_{k-1}^{\tilde{z}} + \tilde{z}_{k\|k-1}\ \tilde{z}_{k\|k-1}^T}{1+\rho} & ; k > 0 \end{cases}$
	$N_k = E_k^{\tilde{z}} - P_{xz,k\|k-1}^T P_{xx,k\|k-1}^{-1} Q_{k-1} P_{xx,k\|k-1} P_{xz,k\|k-1} - \beta R_k$
	$M_k = P_{zz,k\|k-1} - E_k^{\tilde{z}} + N_k + (\beta - 1) R_k$
	$c_k = \dfrac{trace(N_k)}{trace(M_k)}$
	$\lambda_k = \max\{c_k, 1\}$
ST-based Correction:	$P_{xx,k\|k-1}^{ST} = \lambda_k \left(P_{xx,k\|k-1} - Q_{k-1}\right) + Q_{k-1}$
	$P_{xx,k\|k-1}^{ST} = (S_{k\|k-1}^{ST})^T S_{k\|k-1}^{ST}$
	$X_j^{SN,QL} = \phi^{-1}\left(x_{j,d^*}^{L,Shifted}\right);\ j = 0, 1, 2, \dots, N-1$
	$X_{j,k\|k-1}^{ST,QGL} = \hat{x}_{k\|k-1} + S_{k\|k-1}^{ST} X_j^{SN,QL}\ ; j = 0, 1, 2, \dots, N-1$
	$\hat{z}_{k\|k-1}^{ST} \approx \frac{1}{N}\sum_{j=0}^{N-1} h\left(X_{j,k\|k-1}^{ST,QGL}, u_k\right)$
	$P_{zz,k\|k-1}^{ST} \approx \frac{1}{N}\sum_{j=0}^{N-1} \left[h\left(X_{j,k\|k-1}^{ST,QGL}, u_k\right) - \hat{z}_{k\|k-1}^{ST}\right]$
	$* \left[h\left(X_{j,k\|k-1}^{ST,QGL}, u_k\right) - \hat{z}_{k\|k-1}^{ST}\right]^T + R_k$
	$P_{xz,k\|k-1}^{(iter)} \approx \frac{1}{N}\sum_{j=0}^{N-1} \left[X_{j,k\|k-1}^{ST,QGL} - \hat{x}_{k\|k-1}\right]$
	$* \left[h\left(X_{j,k\|k-1}^{ST,QGL}, u_k\right) - \hat{z}_{k\|k-1}^{ST}\right]^T$
SI-based update:	$H_k^{pinv} = P_{xx,k\|k-1}^{ST}\left(P_{xz,k\|k-1}^{ST}(P_{xz,k\|k-1}^{ST})^T\right)^{-1} P_{xz,k\|k-1}^{ST}$
	$G_k^{silf} = H_k^{pinv} Sat^{diag}\left(\dfrac{\left\|z_k - \hat{z}_{k\|k-1}^{ST}\right\|}{\delta}\right)$
	$\hat{x}_{k\|k} = \hat{x}_{k\|k-1} + G_k^{silf}(z_k - \hat{z}_{k\|k-1}^{ST})$
	$P_{xx,k\|k} = P_{xx,k\|k} - G_k^{silf} P_{zz,k\|k-1}^{ST} (G_k^{silf})^T$
Iterative Strategy:	Initialize statistical moments for $iter = 1$, $\hat{x}_{k\|k}^{(1)} = \hat{x}_{k\|k}$, $P_{xx,k\|k}^{(1)} = P_{xx,k\|k}$, and set $iter = 2$
	Repeat (22)-(30) of the iterative filtering strategy presented in section III.B until the specified stop criterion is met.

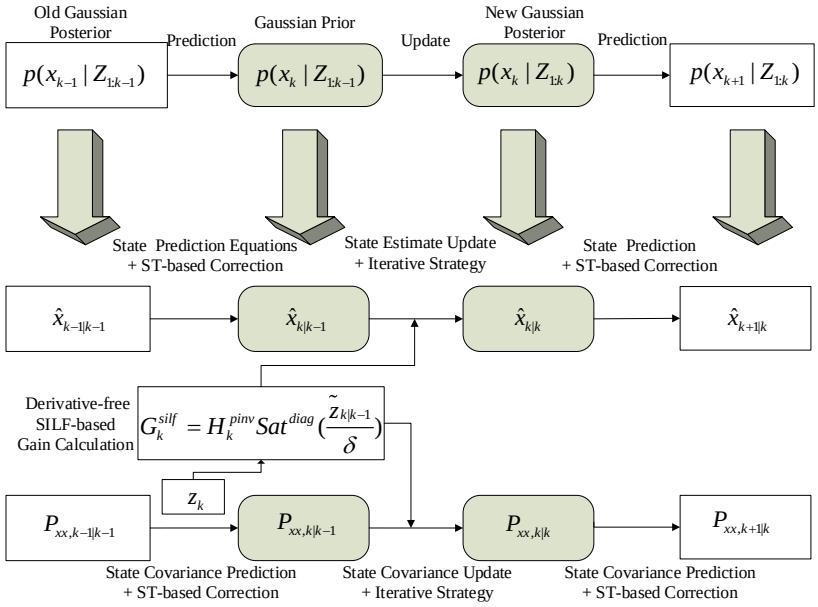

Fig. 1. Flowchart of the proposed RLKF algorithm

where $I_{n\times n}$ is $n \times n$ identity matrix that represents the system transition matrix. In this study, the nonlinear measurement model contains $r = 5$ harmonic orders (including 1st, 3rd, 5th, 7th, and 11th order) that matches with the harmonic contents (with considerable amplitudes) of power signals in smart power grids in most cases.

To demonstrate the strength of the proposed filtering strategy in various operating modes, different scenarios of simulations along with experiments have been implemented. As per software simulations, two harmonic estimation problems are defined for estimating the harmonic parameters of static and dynamic (with time-varying amplitude) signals. As per practical applications of the proposed method, an experimental setup has been mounted to evaluate the performance of the proposed filters under the switching operating mode of the power system (abrupt changes of the power signal). In fact, the proposed methods are applied to process the transient logged data set so that their harmonic parameters are estimated. Then, the estimated waveform is constructed using the estimated harmonic contents. Finally, the proposed algorithms are implemented in a real-time hardware-in-the-loop (HIL) setup for evaluating their robustness and accuracy in practical applications. The performance of the proposed RLKF and SILF in terms of accuracy, robustness, and computational complexity is compared to those of conventional UKF, EKF, Extended SIF (ESIF), and original LKF as well.

Note that for all scenarios, the initial state vector and state error covariance matrix are set to $\hat{x}_0 = [0]_{n\times 1}$and $P_0 = 10^3 \times I_{n\times n}$, respectively; also, system and measurement noise covariance are set to $\mathrm{Q} = 10^{-10} \times I_{n\times n}$ and $\mathrm{R} = 4 \times 10^{-4}$, respectively. The sliding boundary layer δ for all simulations and experiments is between 0.02 and 0.2, whose value has been selected according to the theoretical bound presented by [20]. The forgetting factor ρ and softening factor β (related to strong tracking strategy) are set to 0.95 and 4.5, respectively. Moreover, the sampling frequency of 1200 Hz (24 samples per cycle of power signal) has been considered for all simulations. Note that in all scenarios the iterated stage of RLKF is executed only for one iteration.

A. *Scenario 1: Static Power Signal Estimation*

In this section, the reference signal is considered as a distorted waveform defined as a series of 5 common harmonic contents, which matches with the electrical current of arc furnaces and high-intensity discharge electronic devices [36]:

$$z_k = 1.5sin(\omega t + 80°) + 0.5sin(3\omega t + 60°) \ldots$$
$$+0.2sin(5\omega t + 45°) + 0.15sin(7\omega t + 36°) \ldots$$
$$+0.1sin(11\omega t + 30°) + v_k \quad (40)$$

wherein ω denotes the angular frequency of the fundamental harmonic component of the power signals whose frequency is 50Hz in our study. The static signal defined in (40) is used to assess the capabilities of the proposed filtering methods (RLKF and ISILF) in tracking the original signal corrupted with noise v_k (white noise). Accordingly, two different levels of noise with signal-to-noise ratios (SNRs) of 30dB and 20dB are added to the reference signal to investigate the performance of the proposed algorithms in noise rejection. The estimation results of the proposed RLKF and ISILF are compared with those obtained by the UKF, ESIF, and original LKF. Note that the initial parameters of all filters are set to the same values for all noisy conditions. Due to space limitations, only the graphical representations of the estimation results obtained by the filtering methods for the highest noise level (SNR = 20dB) are presented. The standard deviation of the Gaussian noise i.e., v_k injected to the static waveform in (40) is set to be 0.022.

Regardless of the relatively lower convergence rate of the proposed algorithms in estimating parameters of the higher-order (harmonic) components (as seen in Fig. 2), RLKF and

ISILF track the overall waveform with a convergence time of around half a cycle of the power signal, as shown in Fig. 3.a. Note that RLKF presents a better convergence behavior than SILF. Moreover, the proposed estimation algorithms show stability after being converged to the final values of the parameters as shown in Fig. 3. Then, the signal estimation errors introduced by the different algorithms are statistically analyzed and the mean squared error (MSE) and variance (Var) are computed using which the algorithms' accuracy and robustness can be evaluated, respectively. These statistical indices are generated using the estimation results obtained between 0.06s and 0.5s (as discussed, this range is selected to compare the performance of all algorithms after transient behavior of all filters) for all algorithms under various noisy conditions. The results of the first three cycles are not considered to let all algorithms converge to their final values (although this convergence rate of LKF and UKF is not acceptable from the power system operation point of view). Results presented in Table II demonstrate that RLKF and ISILF track the true signal with high accuracy at different noise levels, with RLKF presenting a slightly better result due to the strong tracking strategy integrated with ISILF. As observed from the last column of Table II, the computational complexity of proposed algorithm is dominated by the number of states (n) and the number of lattice points (N), as can be seen from the term n^2N. This means that as the number of states and the number of lattice points increase, the computational burden of the approach rises quadratically with respect to the number of states and linearly with respect to the number of lattice points. Therefore, this approach might face scalability issues when applied to very high-dimensional systems or when a very large number of lattice points is required. However, many of the computations can potentially be parallelized in practical applications, which could significantly reduce the actual computational time if parallel computing resources are available.

Although SILF shows almost the same behavior as the RLKF in tracking the static signal (see Fig. 3), the indices, mean squared error (MSE) and variance (Var), presented in Table II, reveal the lower performance of SILF compared to RLKF. The corresponding results obtained by ESIF are noticeably worse in terms of accuracy and robustness. This is mainly because of the drawback of approximating a highly nonlinear measurement function using the first term of Taylor series expansion. Furthermore, estimation results obtained by UKF and LKF are the worst ones with UKF presenting slightly a better result. As discussed earlier, the required number of sampling points used by LKF increases for approximating functions with a higher level of nonlinearity in the presence of uncertainty (this is why N is set to 21 for LKF). Meeting this requirement is facilitated by an adjustable number of sampling points introduced by the lattice-based filtering strategy. Note that we exploit this capability originated in LKF formulation and improved the performance of the proposed RLKF and ISILF by increasing their number of sampling points (see the results of RLKF and ISILF in Table II where $N = 21$).

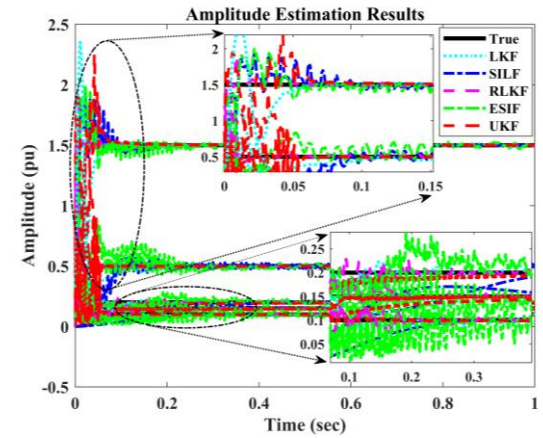

(a)

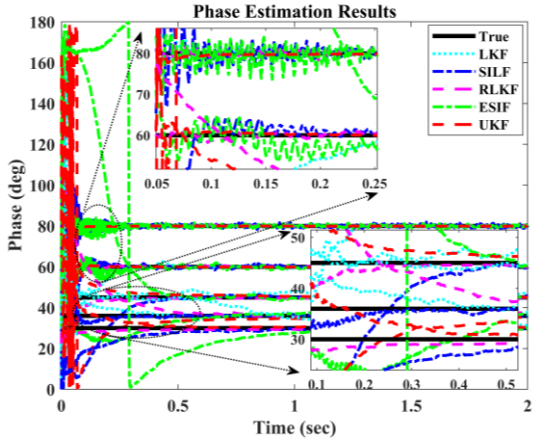

(b)

Fig 2. (a) Amplitude and (b) phase estimation results obtained by different algorithms for the static waveform.

B. *Scenario 2: Dynamic Power Signal*

Time-varying operating conditions in the power systems yield some dynamic changes in the electrical waveforms. These dynamics cause time-varying harmonic parameters whose estimation would be more challenging. In this subsection, we define a dynamic power signal by injecting time-variant terms into the signal (40), using which the performance of the proposed algorithms is further investigated for dynamic signal tracking. The following equation represents the dynamic signal with the corresponding time-variant parameters:

$$\begin{aligned} Z_k = {} & \big(1.5 + \mathrm{a}_1(t)\big)sin(\omega t + 80°) + \cdots \\ & \big(0.5 + \mathrm{a}_3(t)\big)sin(3\omega t + 60°) + \cdots \\ & \big(0.2 + \mathrm{a}_5(t)\big)sin(5\omega t + 45°) + \cdots \\ & 0.15sin(7\omega t + 36°) + 0.1sin(11\omega t + 30°) + v_k \end{aligned} \quad (41)$$

where

$$\begin{aligned} \mathrm{a}_1(t) &= 0.15sin(2\pi \mathrm{f}_1 t) + 0.05sin(2\pi \mathrm{f}_3 t), \\ \mathrm{a}_3(t) &= 0.05sin(2\pi \mathrm{f}_2 t) + 0.02sin(2\pi \mathrm{f}_3 t) \\ \mathrm{a}_5(t) &= 0.025sin(2\pi \mathrm{f}_1 t) + 0.005sin(2\pi \mathrm{f}_3 t) \\ \mathrm{f}_1 &= 0.25 + 1.875\mathrm{t}\ \mathrm{Hz} \\ \mathrm{f}_2 &= 0.75 + 5.625\mathrm{t}\ \mathrm{Hz} \\ \mathrm{f}_3 &= 1.5 + 11.25\mathrm{t}\ \mathrm{Hz} \end{aligned}$$

TABLE II
STATISTICAL COMPARISON OF FILTERS IN ESTIMATING STATIC SIGNAL

	Number of Points	SNR (dB) 30 MSE	30 Var	20 MSE	20 Var	Average Time (sec) 2 sec sim.	Computational Complexity (FLOPs)
UKF	$2n+1 = 21$	6.0395×10^{-4}	4.4639×10^{-4}	6.1409×10^{-3}	4.3697×10^{-3}	0.4180	$O(n^3 + n^2m)$
ESIF	-	1.1502×10^{-3}	8.9456×10^{-4}	5.4242×10^{-3}	4.3438×10^{-3}	0.2758	$O(n^3 + m^3)$
PFSIF	$P = 1000$	8.2341×10^{-4}	4.7658×10^{-4}	5.7312×10^{-3}	3.6454×10^{-3}	1.8671	$O(PlogP + Pn)$
LKF	$N = 21$	8.9149×10^{-4}	7.3073×10^{-4}	6.9803×10^{-3}	5.7631×10^{-3}	0.3973	$O(n^3 + n^2N)$
SILF	$N = 21$	2.5654×10^{-4}	1.1449×10^{-4}	7.8205×10^{-4}	5.1438×10^{-4}	0.4207	$O(n^3 + n^2N)$
	$N = 11$	8.6804×10^{-4}	5.4786×10^{-4}	5.1592×10^{-3}	3.0522×10^{-3}	0.3427	
RLKF	$N = 21$	1.8741×10^{-4}	9.1593×10^{-5}	6.0078×10^{-4}	4.6312×10^{-4}	0.4288	$O(iter(n^3 + n^2N))$
	$N = 11$	7.7928×10^{-4}	6.1528×10^{-4}	4.5894×10^{-3}	1.9837×10^{-3}	0.3657	

n is the number of states; *m* is number of measurements; *N* is the number of lattice points; and *P* is the number of particles for PFSIF; *iter* is number of iterations.

As seen, the amplitudes of 1st, 3rd, and 5th harmonics are considered to be time-varying signals with time-dependent frequencies as well which makes the harmonic estimation problem even more complex. Additionally, a 20 dB Gaussian noise (zero-mean with standard deviation = 0.022) is added to make the model represents real-world conditions.

Figs. 4 and 5 demonstrate the harmonic parameters and the associated dynamic signal estimated by the filtering algorithms along with their corresponding estimation errors. although the filters are blind to these dynamic changes of the signal due to the fact that their process model formulation is kept similar to one defined for the static signal in (41), as can be observed, the proposed SILF and RLKF maintained their estimation quality in the presence of model dynamics. However, the convergence rate of the estimation problem in this scenario is slightly lower than that of the static signal case.

It should be noted that the performance of UKF and LKF estimators significantly declined in tracking the dynamic signal; on the other hand, ESIF results remain acceptable benefiting from the sliding innovation strategy in its formulation. Table III presents the performance of the proposed algorithms in comparison with other filtering methods in terms of statistical indices: MSE and Var. These indices are again computed using the estimated value of the dynamic waveform obtained between 0.06s and 0.5s for all algorithms. As per the estimation results given in this table, UKF and LKF present the highest errors among the others. Although ESIF performance is comparable to that of SILF and RLKF with 11 sampling points, the proposed algorithms with 21 sampling points clearly outperform ESIF but at a higher computational cost. Note that PFSIF also present comparable results to those obtained by proposed algorithms with 11 points but with significantly higher computational burden (1000 particles). This superiority of the SILF and RLKF originates in the fact that the sliding innovation strategy (used by both) and strong tracking theory (adaptive fading factor used in RLKF) place more weight on the measurements than the process model when encountering model uncertainties.

C. *Scenario 3: Power Signal with Abrupt changes*

Transient phenomena in power systems yield abrupt changes in the power signals with an effective time in the range of a few microseconds to milliseconds. Such a sudden change in the power signal introduces some challenges to the filtering algorithms in maintaining their robustness while tracking the transient waveform.

In this section, an experimental setup (shown in Fig. 6) is developed to extract data under a transient phenomenon, i.e., load switching. We then apply the SILF, RLKF, and ESIF algorithms to estimate the voltage magnitudes with transient changes measured from the test setup.

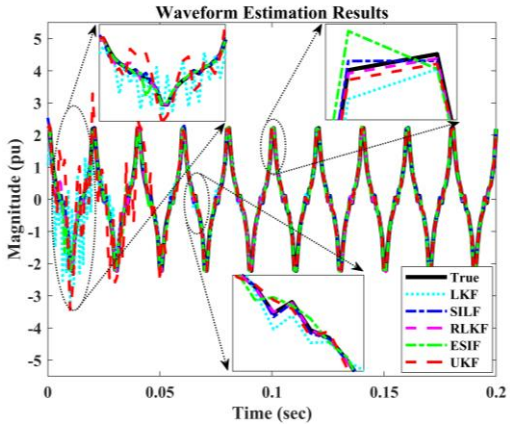

(a)

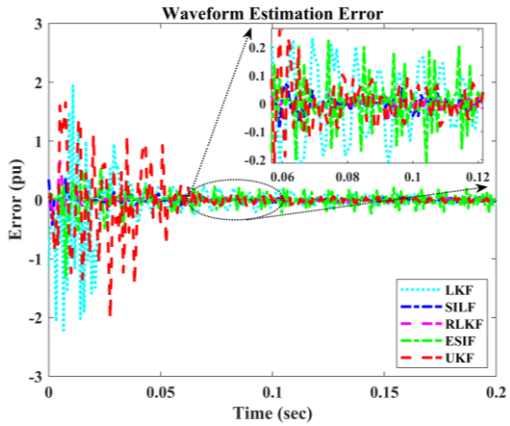

(b)

Fig 3. (a) Estimated waveform and (b) the corresponding error of different algorithms for static signal.

This article has been accepted for publication in IEEE Open Journal of Signal Processing. This is the author's version which has not been fully edited and content may change prior to final publication. Citation information: DOI 10.1109/OJSP.2023.3298555

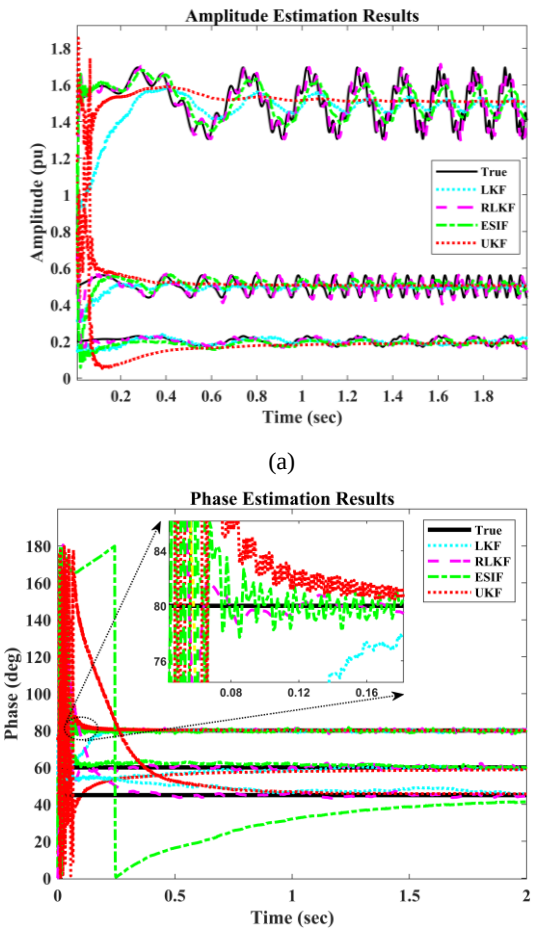

Fig 4. (a) Amplitude and (b) phase estimation results obtained by different algorithms for the dynamic waveform.

TABLE III
STATISTICAL COMPARISON OF FILTERS IN TRACKING DYNAMIC SIGNAL

	Number of Points	SNR (dB) 20	
		MSE	Var
UKF	21	2.3578×10^{-2}	1.1798×10^{-2}
ESIF	-	9.1090×10^{-3}	5.8768×10^{-3}
PFSIF	1000	5.7581×10^{-3}	3.4377×10^{-3}
LKF	21	3.8375×10^{-2}	2.7631×10^{-2}
SILF	21	9.4805×10^{-4}	7.1438×10^{-4}
	11	7.3592×10^{-3}	6.0522×10^{-3}
RLKF	21	6.9759×10^{-4}	3.5671×10^{-4}
	11	5.1894×10^{-3}	4.6837×10^{-3}

The mounted circuit consists of a 0.1H inductor connected in series with two parallel transformers whose named power are 100VA and 200VA, respectively. The 100VA transformer operates under the no-load condition and is directly supplied via an AC power source; however, the 200VA transformer is fed through a switch to supply a 48W LED driver load. A fast response voltage transducer, i.e., LV 25-P, is used to measure the analog voltage of the series inductor. The analog data is then digitized using an A/D NI USB-6009 data acquisition (DAQ) card at a sampling rate of 1200 Hz. Transient voltage change of the series inductor is generated by switching the 200VA transformer (supplying LED load on its secondary winding) at the time of 2.759sec. Fig. 6 also depicts the transient changes of inductor voltage after switching time. Note that the filtering algorithms are used in the off-line mode to process the logged data of transient voltage waveform.

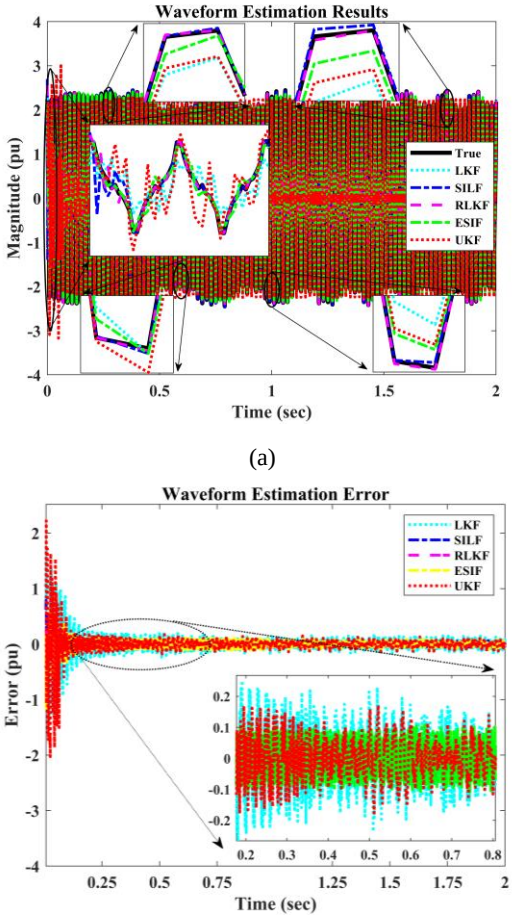

Fig 5. (a) Estimated waveform and (b) the corresponding error of different algorithms for the dynamic signal.

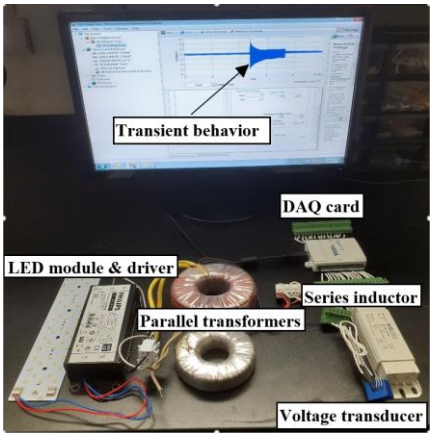

Fig. 6. Experimental setup for testing abrupt changes in the signal.

Fig. 7 shows the graphical representation of their corresponding estimated signals. As observed, RLKF tracks the measured transient waveform within an acceptable range of

error compared to other algorithms. Since transient changes in the signal are not modeled in the process model of the filtering algorithms, their predicted results in the time update phase present a significant error. Using UKF and LKF algorithm, this error is propagated to the measurement update phase which yields low-quality updated estimates. On the other hand, SILF and RLKF exploit the sliding innovation strategy in their measurement update phase to compensate for the errors of the time update phase. This robust behavior against sudden changes is reinforced for RLKF by exploiting an adaptive fading factor term applied to the predicted error covariance. Thus, RLKF provides even more reliable estimation results for transient changes in the system model. The estimation results obtained by estimators are compared numerically in Table IV. As discussed above (and even could be predicted from dynamic case results), UKF and LKF poorly track the abrupt changes, and this is why we exclude them in reporting the results in this section.

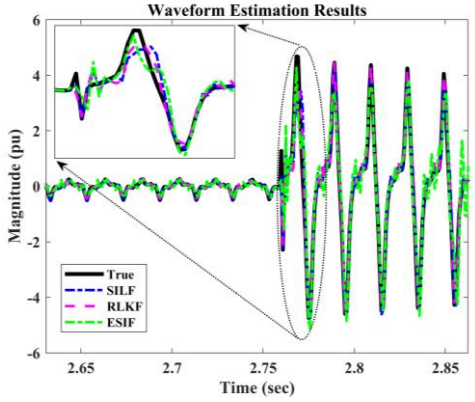

(a)

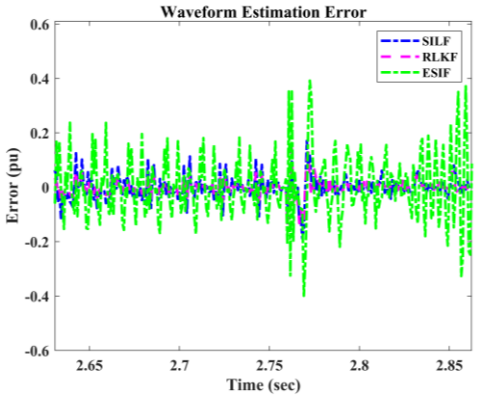

(b)

Fig. 7. (a) Estimated waveform and (b) the corresponding error of different algorithms for transient signal.

D. Scenario 4: Real-time Implementation

In this section, a Hardware-In-the-Loop (HIL) setup is developed to evaluate the real-time operation of the proposed SILF and RLKF methods. Since MATLAB-based implemented scripts present some processing delays while reading data from DAQ cards, the C++ programming language, which provides strong traction in real-time applications, is used in the current scenario for the implementation of the proposed algorithms. The codes are processed in a real-time manner using an embedded hardware system, i.e., PC/104 micro-computer set, equipped with a VDX-6354 processor card (Vortex86DX 800MHz CPU module) and a PCM-5114 DAQ card. Furthermore, we employ a fast response current sensor using which the current of an AC feeder line supplying a total of 6KW LED luminaires is measured. This current is then read by the DAQ card at the sampling rate of 1200 Hz. The harmonic contents of the measured current are 3rd, 5th, and 7th harmonic orders with noticeable amplitude. Fig. 8 shows the diagram of the real-time experimental setup.

TABLE IV
STATISTICAL COMPARISON OF FILTERS IN TRACKING SIGNAL WITH ABRUPT CHANGE

	Number of Points	MSE	Var
ESIF	-	5.5655×10^{-2}	4.2975×10^{-3}
SILF	21	7.8734×10^{-3}	5.9583×10^{-3}
	11	3.8885×10^{-2}	2.5487×10^{-2}
RLKF	21	4.3759×10^{-3}	1.1006×10^{-3}
	11	2.2804×10^{-2}	9.0337×10^{-3}

Once a measurement is received by the DAQ card, a 5V digital activation pulse is submitted to the General-Purpose Input Output (GPIO) port of the processor card and one recursion of the filtering method (SILF or RLKF) is simultaneously executed to provide the estimates associated with the current recursion. The digital pulse is then set to 0V at the end of each recursion of the corresponding estimator. The train of pulses detected by a digital scope is then used to analyze the computational performance of the proposed algorithms. To guarantee the real-time performance of the proposed methods, the duration of the digital activation pulse (processing time) is required to be less than $(1/1200)s$ (since the sampling rate is 1200Hz). As Figs. 9.a and 9.b depicts, the processing time of all recursions (not exactly the same though) is always less than $(1/3000)s$ and (1/2500)s for SILF and RLKF, respectively, which confirms the performance of the proposed algorithms in real-time applications. Note that the number of lattice-based sampling points for both algorithms is set to 21. It is worth mentioning that the relatively low computational burden of SILF originates in using a simple integration method (Lattice rule) to approximate nonlinear multivariate integrals (inherited from LKF), and a simple gain formulation inherited from SIF. Having the SILF formulation reinforced by the iterative filtering strategy and strong tracking filtering method, RLKF provides more robust and accurate estimation results but at a higher computational complexity.

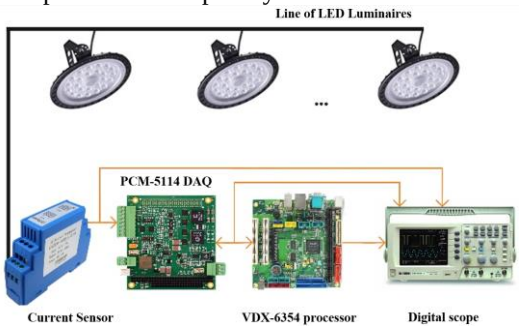

Fig. 8. Real-time HIL experimental setup.

The estimated waveform is outputted by the DAQ card to its analog output channel (for each proposed filter). Then, the measured and estimated waveforms are cabled to the scope. Note that for the sake of a more efficient graphical representation, the data logged for 1-minute execution of the SILF and RLKF algorithms is used in the MATLAB environment to present the measured and estimated waveforms in one plot, as shown in Fig. 9.c.

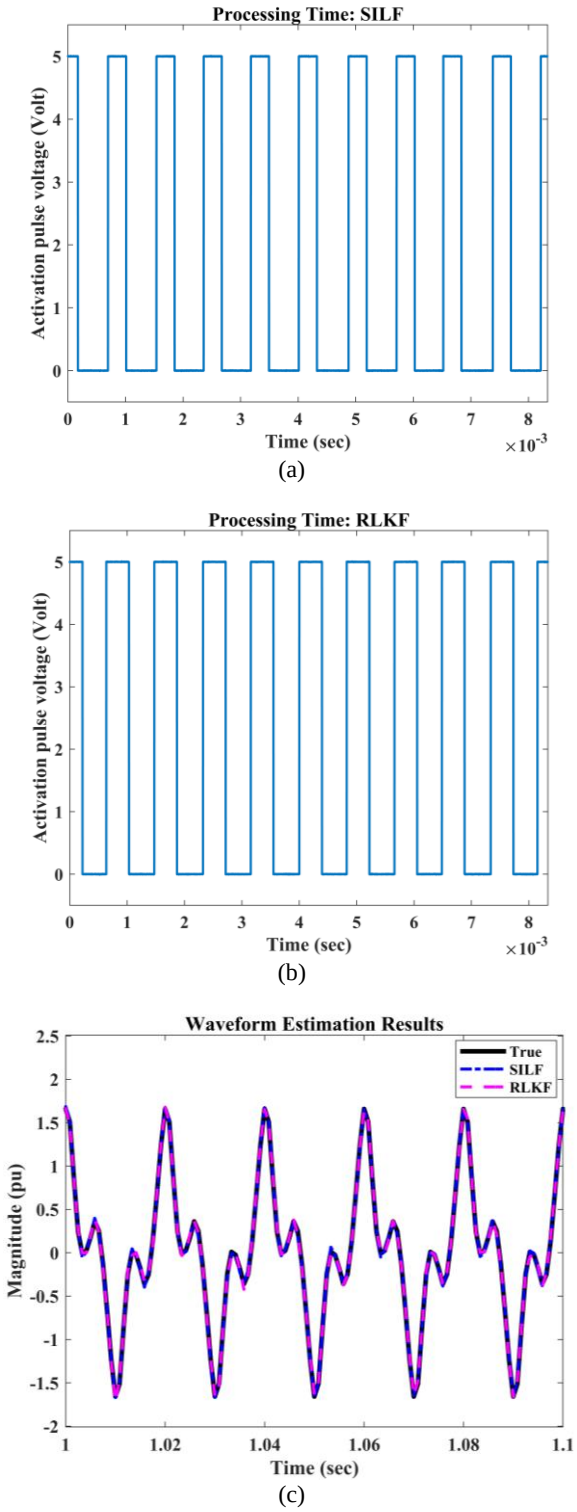

Fig. 9. Processing time of (a) SILF and (b) RLKF along with (c) their real-time estimation results.

TABLE V
STATISTICAL COMPARISON OF THE PROPOSED FILTERS IN REAL-TIME APPLICATION

	Number of Points	MSE	Var
SILF	21	8.2767×10^{-4}	6.5874×10^{-4}
RLKF	21	6.1286×10^{-4}	3.2322×10^{-4}

V. CONCLUSIONS

This paper presented a derivative-free robust formulation of the LKF algorithm, namely SILF, by applying the sliding innovation strategy to the update stage of the original method with the aim of enhancing its performance against different uncertainty resources. The proposed algorithm was then reinforced by an adaptive fading factor and iterated filtering method to battle transient changes in the system model/parameters. The resulting filter has been formulated as a predictor-corrector estimator and is called RLKF. Different simulation and experiment scenarios have been carried out to investigate the performance of the proposed SILF and RLKF under uncertain system dynamics perturbed with high-level noises as well. The obtained results have shown the superiority of the RLKF compared to SILF, ESIF, UKF, and the original LKF in terms of accuracy and robustness, and convergence rate as well. Furthermore, the results obtained from a HIL setup based on real-time coding and an embedded hardware system have confirmed the performance of the proposed filtering strategy in the real-time application in terms of estimation accuracy and processing time. Although RLKF requires more computational burden compared to SILF and other well-known filtering methods, its adjustable number of sampling points inherited from the LKF formulation gives us the opportunity of reducing the number of points for the systems with a lower level of nonlinearity and uncertainty while maintaining the estimation accuracy in an acceptable range. The development of the proposed filter in the non-Gaussian framework and its interacting multiple models (IMM)-based formulation for fault tolerance and detecting model changes are considered for future research works.

REFERENCES

[1] R. E. Kalman, “A new approach to linear filtering and prediction problems,” 1960.

[2] M. I. Ribeiro, “Kalman and extended kalman filters: Concept, derivation and properties,” *Institute for Systems and Robotics*, vol. 43, p. 46, 2004.

[3] J. L. Crassidis and J. L. Junkins, *Optimal estimation of dynamic systems*. Chapman and Hall/CRC, 2004.

[4] S. J. Julier and J. K. Uhlmann, “Unscented filtering and nonlinear estimation,” *Proceedings of the IEEE*, vol. 92, no. 3, pp. 401–422, 2004, doi: 10.1109/JPROC.2003.823141.

[5] S. J. Julier and J. K. Uhlmann, “New extension of the Kalman filter to nonlinear systems,” in *Signal processing, sensor fusion, and target recognition VI*, International Society for Optics and Photonics, 1997, pp. 182–193.

[6] B. Ienkaran Arasaratnam, "CUBATURE KALMAN FILTERING: THEORY & APPLICATIONS." McMaster University, 2012.

[7] A. Rahimnejad, S. A. Gadsden, and M. Al-Shabi, "Lattice Kalman Filters," *IEEE Signal Process Lett*, vol. 28, pp. 1355–1359, 2021, doi: 10.1109/LSP.2021.3089935.

[8] Q. Xia, M. Rao, Y. Ying, and X. Shen, "Adaptive fading Kalman filter with an application," *Automatica*, vol. 30, no. 8, pp. 1333–1338, 1994.

[9] W. Zhou and J. Hou, "A New Adaptive Robust Unscented Kalman Filter for Improving the Accuracy of Target Tracking," *IEEE Access*, vol. 7, pp. 77476–77489, 2019, doi: 10.1109/ACCESS.2019.2921794.

[10] H. Zhang, J. Xie, J. Ge, W. Lu, and B. Zong, "Adaptive Strong Tracking Square-Root Cubature Kalman Filter for Maneuvering Aircraft Tracking," *IEEE Access*, vol. 6, pp. 10052–10061, 2018, doi: 10.1109/ACCESS.2018.2808170.

[11] D. Simon, *Optimal state estimation: Kalman, H infinity, and nonlinear approaches*. John Wiley & Sons, 2006.

[12] J. Zhao and L. Mili, "A Theoretical Framework of Robust <italic>H</italic>-Infinity Unscented Kalman Filter and Its Application to Power System Dynamic State Estimation," *IEEE Transactions on Signal Processing*, vol. 67, no. 10, pp. 2734–2746, 2019, doi: 10.1109/TSP.2019.2908910.

[13] J. Zhao and L. Mili, "A Decentralized H-Infinity Unscented Kalman Filter for Dynamic State Estimation Against Uncertainties," *IEEE Trans Smart Grid*, vol. 10, no. 5, pp. 4870–4880, 2019, doi: 10.1109/TSG.2018.2870327.

[14] J. Xia, S. Gao, X. Qi, J. Zhang, and G. Li, "Distributed cubature H-infinity information filtering for target tracking against uncertain noise statistics," *Signal Processing*, vol. 177, p. 107725, 2020, doi: https://doi.org/10.1016/j.sigpro.2020.107725.

[15] S. R. Habibi and R. Burton, "The Variable Structure Filter," *J Dyn Syst Meas Control*, vol. 125, no. 3, pp. 287–293, Sep. 2003, doi: 10.1115/1.1590682.

[16] S. A. Gadsden and B. M. Eng, "SMOOTH VARIABLE STRUCTURE FILTERING: THEORY AND APPLICATIONS."

[17] S. A. Gadsden, M. Al-Shabi, I. Arasaratnam, and S. R. Habibi, "Combined cubature Kalman and smooth variable structure filtering: A robust nonlinear estimation strategy," *Signal Processing*, vol. 96, pp. 290–299, 2014.

[18] I. Al-Omari, A. Rahimnejad, A. Gadsden, M. Moussa, and H. Karimipour, "Power System Dynamic State Estimation Using Smooth Variable Structure Filter," in *2019 IEEE Global Conference on Signal and Information Processing (GlobalSIP)*, 2019, pp. 1–5. doi: 10.1109/GlobalSIP45357.2019.8969306.

[19] M. Avzayesh, M. Abdel-Hafez, M. AlShabi, and S. A. Gadsden, "The smooth variable structure filter: A comprehensive review," *Digit Signal Process*, vol. 110, p. 102912, 2021, doi: https://doi.org/10.1016/j.dsp.2020.102912.

[20] A. S. Lee, "Sliding Innovation Filtering: Theory and Applications."

[21] S. A. Gadsden and M. Al-Shabi, "The sliding innovation filter," *IEEE Access*, vol. 8, pp. 96129–96138, 2020.

[22] W. Hilal, S. A. Gadsden, S. A. Wilkerson, and M. Al-Shabi, "Combined particle and smooth innovation filtering for nonlinear estimation," in *Signal Processing, Sensor/Information Fusion, and Target Recognition XXXI*, SPIE, 2022, pp. 29–42.

[23] J. Enayati, A. Rahimnejad, L. Vanfretti, S. A. Gadsden, and M. Al-Shabi, "Dynamic Harmonic Estimation Using a Novel Robust Filtering Strategy: Iterated Sliding Innovation Cubature Filter," *IEEE Trans Instrum Meas*, vol. 72, pp. 1–10, 2023, doi: 10.1109/TIM.2022.3218539.

[24] T. Zhang, W. Zhang, Q. Zhao, J. Chen, and Y. Zhang, "Adaptive Particle Filter with Randomized Quasi-Monte Carlo Sampling for Unbalanced Distribution System State Estimation," *IEEE Trans Instrum Meas*, p. 1, 2023, doi: 10.1109/TIM.2023.3276002.

[25] J. Wang, X. Chen, and P. Yang, "Adaptive H-infinite kalman filter based on multiple fading factors and its application in unmanned underwater vehicle," *ISA Trans*, vol. 108, pp. 295–304, 2021, doi: https://doi.org/10.1016/j.isatra.2020.08.030.

[26] A. Rahimnejad, "Lattice Kalman Filters: Theory and Applications." University of Guelph, 2022.

[27] R. Zhan and J. Wan, "Iterated Unscented Kalman Filter for Passive Target Tracking," *IEEE Trans Aerosp Electron Syst*, vol. 43, no. 3, pp. 1155–1163, 2007, doi: 10.1109/TAES.2007.4383605.

[28] A. Rouhani and A. Abur, "Constrained iterated unscented Kalman filter for dynamic state and parameter estimation," *IEEE Transactions on Power Systems*, vol. 33, no. 3, pp. 2404–2414, 2017.

[29] J. Enayati, A. Rahimnejad, and S. A. Gadsden, "LED Reliability Assessment Using a Novel Monte Carlo-Based Algorithm," *IEEE Transactions on Device and Materials Reliability*, vol. 21, no. 3, pp. 338–347, 2021, doi: 10.1109/TDMR.2021.3095244.

[30] D. Nuyens, *Fast construction of good lattice rules*, no. April. 2007.

[31] H. H. Afshari, S. A. Gadsden, and S. Habibi, "Gaussian filters for parameter and state estimation: A general review of theory and recent trends," *Signal Processing*, vol. 135. Elsevier B.V., pp. 218–238, Jun. 01, 2017. doi: 10.1016/j.sigpro.2017.01.001.

[32] H. Fang, N. Tian, Y. Wang, M. Zhou, and M. A. Haile, "Nonlinear Bayesian estimation: From Kalman filtering to a broader horizon," *IEEE/CAA Journal of Automatica Sinica*, vol. 5, no. 2. Institute of Electrical and Electronics Engineers Inc., pp. 401–417, Mar. 01, 2018. doi: 10.1109/JAS.2017.7510808.

[33] R. Cranley and T. N. L. Patterson, "Randomization of Number Theoretic Methods for Multiple Integration," *SIAM J Numer Anal*, vol. 13, no. 6, pp. 904–914, Dec. 1976, doi: 10.1137/0713071.

[34] D. Nuyens, *Fast construction of good lattice rules*, no. April. 2007.

[35] T. Lefebvre, H. Bruyninckx, and J. de Schuller, "Comment on 'A new method for the nonlinear transformation of means and covariances in filters and estimators' [with authors' reply]," *IEEE Trans Automat Contr*, vol. 47, no. 8, pp. 1406–1409, 2002, doi: 10.1109/TAC.2002.800742.

[36] J. Enayati and Z. Moravej, "Real-time harmonic estimation using a novel hybrid technique for embedded system implementation," *International Transactions on Electrical Energy Systems*, vol. 27, no. 12, p. e2428, 2017.

Abolfazl Rahimnejad (Member, IEEE) received the B.Sc. degree from Mazandaran University, Babol, Iran, in 2009, and the M.Sc. degree from the Babol Noshirvani University of Technology, Babol, in 2012, both in electrical power engineering.

From 2013 to 2017, he was a Research Assistant with the Power System Research Laboratory, Babol Noshirvani University of Technology, Mazandaran, Iran. He was then a Visiting Researcher at the Lamar Renewable Energy and Microgrid Laboratory, Beaumont, TX, USA, from 2017 to 2018. After that, he was with the College of Engineering and Physical Sciences, University of Guelph, Guelph, ON, Canada, as a Graduate Research and Teaching Assistant, from 2018 to 2022. He is currently a Research Associate with the Intelligent and Cognitive Engineering Laboratory, McMaster University, Hamilton, ON, Canada. His research interests include estimation and identification methods, data-driven power system operation and control, machine learning Algorithms, and smart home energy management.

Javad Enayati was born in Shahi, Mazandaran, Iran in 1986. He received the B.S. degree in electrical engineering from Mazandaran University, Babol, Iran, in 2009, and M.S. and Ph.D. degrees in electrical power engineering from the Semnan University, Iran, in 2011 and 2017, respectively. From 2016 to 2022, he was with R&D Department of Mazinoor Lighting Industry, Babol, Mazandaran, Iran. Since 2022, he has been post-doctoral research fellow with University of Hertfordshire, Hatfield, UK. His research interests include state estimation, system identification, reliability, and power quality analysis.

Luigi Vanfretti (Senior Member, IEEE) received the M.Sc. and Ph.D. degrees in electric power engineering from the Rensselaer Polytechnic Institute, Troy, NY, USA, in 2007 and 2009, respectively. He was an Associate Professor with the Rensselaer Polytechnic Institute, in 2017, where he is currently developing his laboratory and research team ALSETLab. He was an Assistant Professor, an Associate Professor (tenured), and a Docent with the KTH Royal Institute of Technology, Stockholm, Sweden, from 2010 to 2013 and from 2013 to 2017, respectively, where he led the SmarTS Lab (a research group). He was with Statnett SF, the Norwegian transmission system operator, from 2013 to 2016, as a Special Advisor with the Research and Development Department, and as a Consultant, from 2011 to 2012 and in 2017. His research interests include synchrophasor technology applications, and cyber-physical power system modeling, simulation, stability, and control.

Stephen Andrew Gadsden (M'09, SM'19) is an Associate Professor in the Department of Mechanical Engineering at McMaster University and is Director of the Intelligent and Cognitive Engineering (ICE) Laboratory. His research area includes control and estimation theory, artificial intelligence and machine learning, and cognitive systems. Dr. Gadsden completed his Bachelors in Mechanical Engineering and Management (Business) and then earned his PhD in Mechanical Engineering at McMaster in the area of estimation theory with applications to mechatronics and aerospace systems. He worked as a postdoctoral researcher for nearly three years at the Centre for Mechatronics and Hybrid Technology (Hamilton, Ontario). He also worked concurrently as a Project Manager in the pharmaceutical industry. Before joining McMaster University, Dr. Gadsden was an Associate/Assistant Professor at the University of Guelph and an Assistant Professor in the Department of Mechanical Engineering at the University of Maryland, Baltimore County (USA). He worked and continues to work with a number of colleagues in NASA, the US Army Research Laboratory (ARL), US Department of Agriculture (USDA), and the National Institute of Standards and Technology (NIST). Dr. Gadsden is an elected Fellow of ASME, is a Senior Member of IEEE, and is a Professional Engineer of Ontario. He is also a certified Project Management Professional (PMP). Dr. Gadsden is a reviewer for a number of ASME and IEEE journals and international conferences.

Mohammad Al-Shabi (Senior Member, IEEE) received the B.Sc. and M.Sc. degrees in mechatronics from the Mechanical Engineering Department, Jordan University for Science and Technology (Jordan), and the Ph.D. degree in mechanical engineering from McMaster University (Canada). His thesis was in the area of filtering and estimation on mechatronic systems. He is currently an Assistant Professor with the Department of Mechanical and Nuclear Engineering, University of Sharjah, United Arab Emirates (UAE). His research areas are broad and consider nonlinear and robust control, filtering, estimation theory, fault detection, robotics, optimization, and artificial intelligence.